Clay Science 14, 211–218 (2010)

–Paper–

MICROSCOPIC STRUCTURE AND SPECTROSCOPIC PROPERTY OF THE SHEAR SURFACE AT THE RESIDUAL STATE OF CLAY

MASAFUMI OKAWARA[a], TAKEHIRO HISATSUNE[b], TOSHIYUKI MITACHI[c] and TAKASHI SAINO[b]

[a] *Faculty of Engineering, Iwate University, Morioka 020-8551, Japan*
[b] *Graduate School of Engineering, Iwate University, Morioka 020-8551, Japan*
[c] *Faculty of Engineering, Nihon University, Narashino 275-8575, Japan*

(Received April 21, 2010. Accepted August 18, 2010)

ABSTRACT

The shear property at the residual state is a very important strength in engineering, as usually used for landslide stability analysis. We examined the microscopic structure of the shear surface and spectroscopic property of adsorbed water. As a result of AFM measurement of shear surface it became clear that shear surface was not a perfect flat, and also by CLSM observation, we found that the contact part of a glass board and a shear surface of clay was only partial contact. It indicates that the area actually touched was smaller than the apparent contact area. The "actual contact area" increased as the normal stress increased. While with FTIR measurement, adsorbed water on shear surface of cohesive soil decreased as the increase in normal stress. In conclusion, the coefficient of residual state shear resistance ($\tan\varphi_r$) of clay can be thought to be the coefficient originated in the increase in the actual contact area caused by the increase in the normal stress.

Key words: Shear strength, AFM, Adsorbed water

INTRODUCTION

The states of the shear have peak state, fully softened state and residual state. Residual state is the steady state that the shear strength converges to a steady minimum value after being suffered a large shear deformation. It is known that the slip surface of landslide formed slicken side is in residual state. Shear strength at the residual state is "residual strength". The residual strength has been used for landslide stability slope analyses and it has been recognized that its measurement is very important in engineering practice. Mitachi et al. (2003) states clearly that the coefficient of shear resistance at the residual state ($\tan\varphi_r$) is the same as the coefficient of shear resistance of Hvorslev ($\tan\varphi_e$) which is thought to be the closest to the true coefficient of shear resistance at present. In other words, "the residual strength is actual shear strength." Thus, we examined shear strength at the residual state. Past studies on residual strength mainly refer to measuring methods, the shear properties and granular materials (ex. Skempton, 1964, 1985; Bishop et al., 1971; Uesugi et al., 1986). For essential discussion of residual strength, the basic way of considering the mechanism is very important. This paper studied the surface properties of shear surface part of the shear property at the residual states. In particular, we focused on 3 points: (1) Roughness of Shear Surface, (2) Actual Contact Area, (3) Spectroscopic Properties of Adsorbed Water. For discussion, a basic concept regarded the mechanism of residual strength of clay based on tribology for friction, wear, and lubrication. On that basis, this paper describes the shear property at the residual state in relation to a basic concept based on tribology. The reason why tribology was introduced in this study stems from the understanding that the shear phenomenon at the residual state is "friction phenomenon."

SAMPLE AND EXPERIMENTAL METHODS

Samples

The sample used in the experiment was "NSF-clay" (New Snow Fine-clay). This clay is popular in geotechnical engineering field in Japan. Table 1 shows physical and mineralogical properties of NSF-clay. This clay is composed of a lot of Pyrophyllite and Quartz. Pyrophyllite is clay mineral and Quartz is mainly composed of sand, so NSF-clay is classified into cohesive soil. The specimen used for the observation of a shear surface was a remolded sample. To make this specimen, the deaerated water was added to powdered NSF-clay and remolded by a blender. Then it was put into a cylindrical acrylics cell and deaerated for 30 minutes, and pre-consolidated for 7 days with the consolidation pressure of 150 kPa.

TABLE 1. Chemical and Physical properties of NSF-clay

Soil particle density: ρ_s	2.78 g/cm^3
Plasticity index: I_P	41.7
Cation Exchange Capacity: CEC	24.5 cmol/kg

Experimental Method

(1) Direct shear box test

The shear surface at the residual state made from a long displacement direct box shear test was used for various experiments (Fig. 1). Conditions of direct box shear test were: Consolidated constant pressure condition, vertical stress = 100 kPa, 200 kPa and 300 kPa; shear displacement = 200 mm; shear speed = 0.5 mm/min.

(2) AFM (Atomic Force Microscope) Measurement

Asperity measurement and surface analysis of shear surface were done by using AFM (Atomic Force Microscope), namely, Veeco Nano Scope III (Fig. 2-a). The measurement range was 10 μm × 10 μm. The procedure was as follows. First, soon after the scanning started, 1 skip line was kept, and each parameter was adjusted so that the concave-convex waveform and error waveform of a reciprocating motion became the same. The sample surface was scanned by a tapping method (Fig. 2-b). Then surface analysis was done from the measured asperity image using the attached software, and the maximum height of the profile (R_{max}), arithmetic mean deviation of the profile (R_a), and increase rate of surface area (RIA) were calculated. Roughness was also quantified by using R_a and RIA. R_a indicates the arithmetic mean deviation of the profile. It is the total area of gray colored in Fig. 3. RIA indicates the increase rate of surface area/against flat surface area. As roughness increases, both R_a and RIA also increase.

(3) CLSM (Confocal Laser Scan Microscope) Observation

The confocal laser scan microscope was used for observing a shear interface. CLSM used for this observation was Bio Rad MRC-1024 (Fig. 4-a). A confocal laser scan microscope irradiates a sample, detects the light or fluorescence reflected from the sample, and with these data, computer makes the image of the sample. The advantage of this microscope is that it only measures the light from the focal plane that passed through a small hole called a "pinhole" (Fig. 4-b). By excluding unnecessary light from the upper and lower sides, comparing with the conventional microscopes, its resolution is improved about 1.4 times, so that clear pictures can be expected. Furthermore, even if a sample is thick, we can obtain optical tomograms of the arbitrary depth because a laser can reach deep. An observation was made on a contact plane of a shear surface and a glass. The shear surface formed by the direct box shear test was cut into a size to fit with an observation

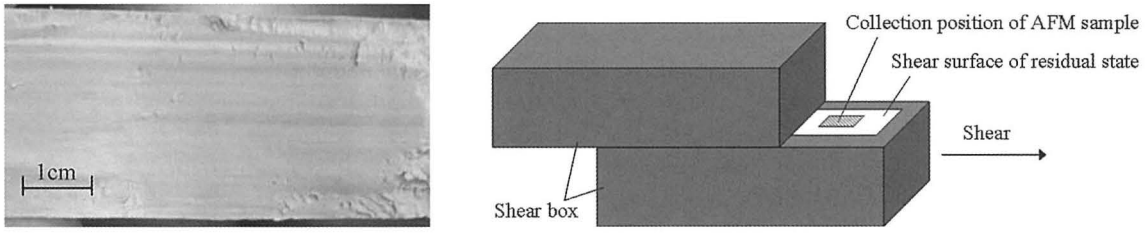

(a) Shear surface at the residual state of NSF-clay (b) Collection position of AFM sample

FIG. 1. The shear surface at the residual state made from a long displacement direct box shear test

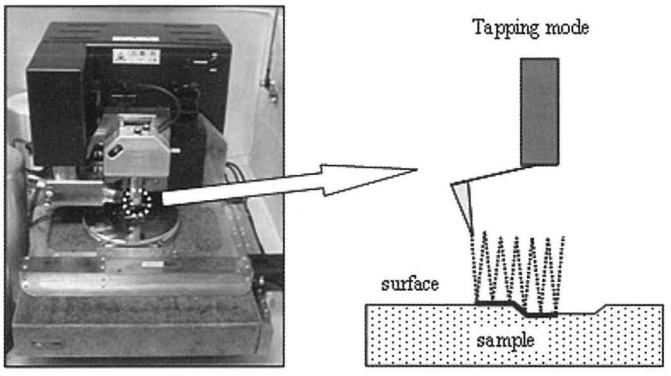

(a) AFM (Veeco Nano Scope-III) (b) Behavior of probe

FIG. 2. AFM and measurement mode

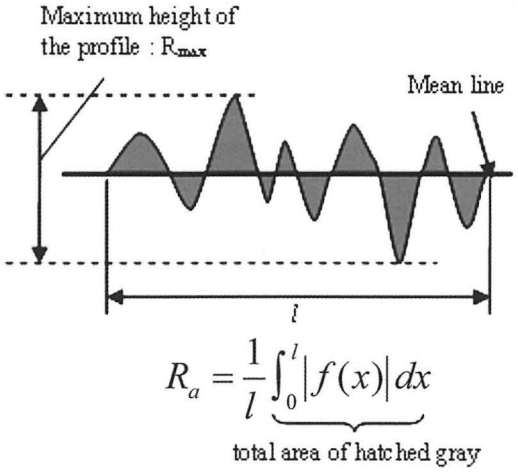

FIG. 3. Index of roughness: R_{max}, R_a

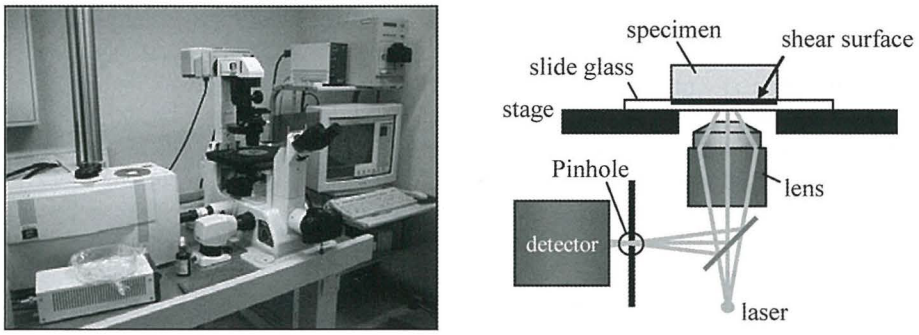

(a) CLSM (Bio-Rad MRC-1024) (b) Observation system

FIG. 4. CLSM and observation method of shear surface

unit. It was then placed and stuck to a tempered glass which was attached at the lower part of the unit. From the glass side, laser was beamed and the contact part of a glass and a shear surface was observed. The conditions of the observation were, reflection, pinhole diameter: 1 mm, laser strength: 3%, image averaging process: 5 times.

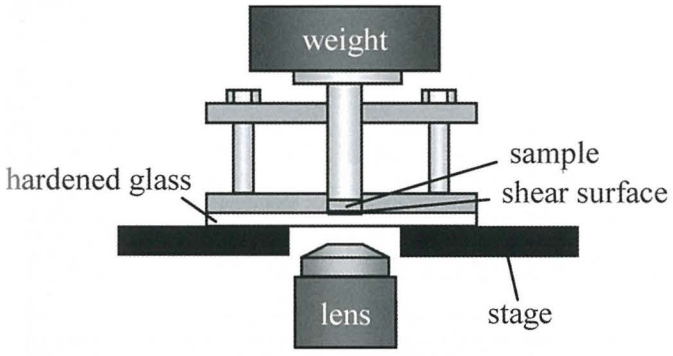

FIG. 5. Overview of a pressure unit

Moreover, a load unit was used to observe the contact surface when adding normal stress. Figure 5 shows the loading method. The normal stress was added by weights.

(4) FTIR (Fourier Transform Infrared Spectrometer) Analysis

In order to clarify the spectroscopic properties of the adsorbed water of a shear surface, it was measured by FTIR (Fourier Transform Infrared Spectrometer). Microscopic-FTIR used for this measurement was JESCO VIR-9500, IR-30 (Fig. 6-a). The measurement was done by ATR that sticks a prism to a sample surface. Microscopic-FTIR excels a local analysis of a sample surface, and also a very small quantity samples. As to this experiment, the diameter was 250 μm, and measurement depth was 250 nm–2000 nm. Background measurement was done first. Subsequently, to perform an infrared spectrum measurement, the shear surface of a sample was touched by a prism of ATR equipment. At this time, the contact pressure of the sample surface and the prism was measured by a small load cell under the sample (Fig. 6-b). Measurement wavenumber domains: 4000 cm^{-1}–400 cm^{-1} of mid-infrared domains, the wavenumber resolution at the time of measurement: 4 cm^{-1}, and the number of addition: 87 times.

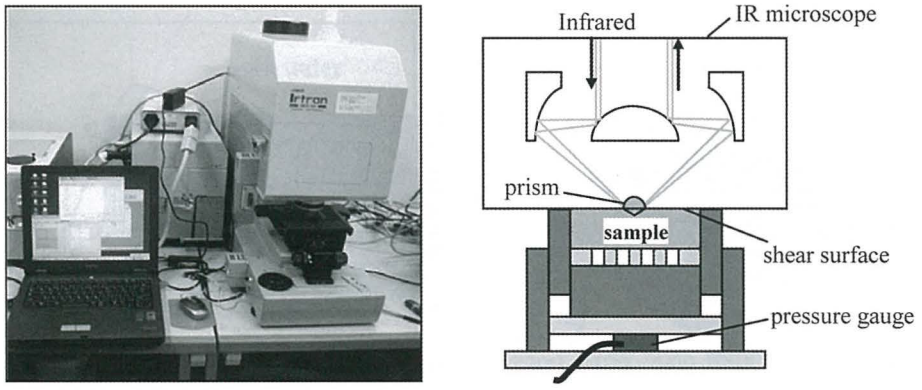

(a) FTIR (Jasco VIR-9500) (b) Attenuated Total Reflection-method (ATR), measuring water content of shear surface according to the changes in normal stress

FIG. 6. FTIR and measurement method of adsorbed water by ATR

EXPERIMENTAL RESULTS AND DISCUSSION

Shear Properties at Residual State

Figure 7 shows residual strength (τ_r') versus vertical stress (σ_V') relationship obtained by large displacement box shear test at dry state and wet state. As shown in the figure, the residual strength differs at dry state and wet state.

Roughness of Shear Surface according to AFM

A concave-convex image of the shear surface at residual state of NSF-clay and a cross-sectional form on ABCD are shown in Figs. 8-a, -b. As shown in these figures, the roughness of the shear surface was confirmed even though the measurement range was very small as to 10 μm × 10 μm. The maximum height of the profile of NSF-clay was R_{max} = 2085 nm, the arithmetic mean deviation was R_a = 284 nm and increase rate of surface area was RIA = 33.67%. A detailed analysis result concerning the surface profile on the shear surface at residual state is described in a past paper (Hisastsune et al., 2008).

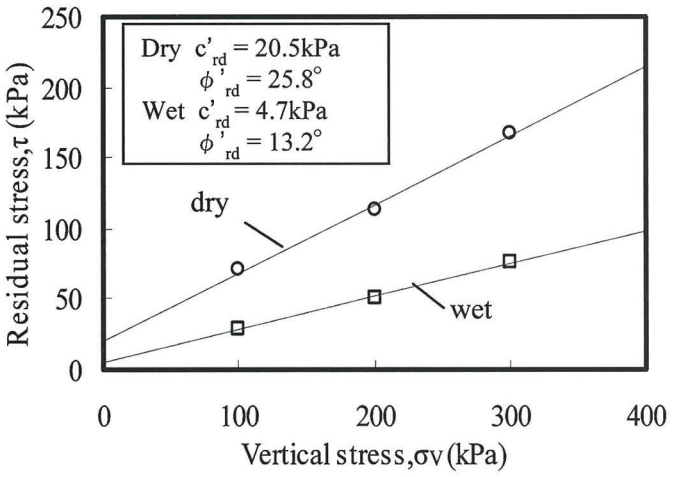

FIG. 7. Comparison of the strength parameter at dry state and wet state on remolded NSF clay

Actual Contact Area according to CLSM

A contact part of a glass board and shear surface of clay was observed from the below by CLSM. Experimentally, we had NSF-clay contact with the glass board. This plane image of the contact part and the cross-sectional image of A–B line are shown in Fig. 9. There is a black ellipse at the center of the image (Fig. 9-a). This part is exactly where the white A–B line is broken in the cross-sectional image (Fig. 9-b). This means that the black portion is a space. That is, the black portion of the planar image is a non-contact region of particles, and in the case of shear surface, water exists here. The planar image of the contact part of the shear surface and the glass is shown in Fig. 10. Different light and dark reflection patterns can be seen on the contact part. If the particles were contacted completely on the shear surface, the image had to be all white. However, the image shows different light and dark patterns, so it is obvious that it was actually contacted only partially. Thus the existence of "the actual contact area" was confirmed. Figure 11 shows when normal stress was increased by a pressure unit. As normal stress was increased gradually (σ_V = 0 kPa, 24.0 kPa, 47.7 kPa, then to 98.4 kPa), the light parts also increased.

Spectroscopic Properties of Adsorbed Water on Shear Surfaces according to FTIR

The infrared spectrum of adsorbed water on shear surface is shown in Fig. 12-a. It also shows the spectrum of the bulk

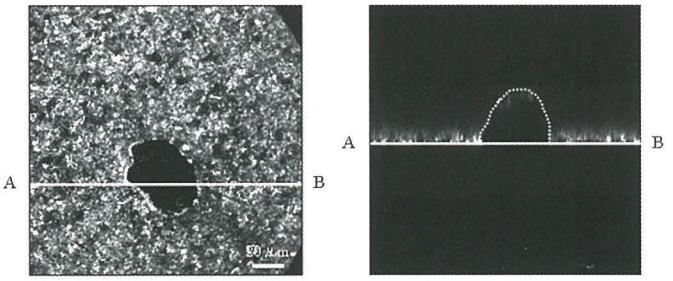

(a) Planar image (b) Cross section image

FIG. 9. CLSM images of contact part of NSF-clay with a glass board

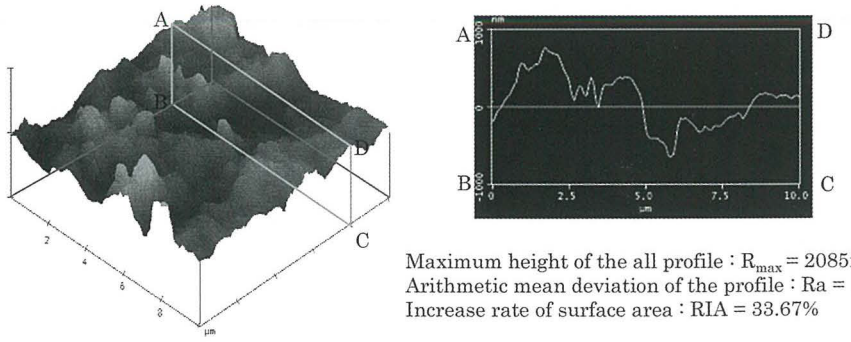

Maximum height of the all profile : R_{max} = 2085nm
Arithmetic mean deviation of the profile : Ra = 284nm
Increase rate of surface area : RIA = 33.67%

(a) 3D image, Right (b) Cross sectional form on ABCD and roughness parameters

FIG. 8. AFM concave-convex image of the shear surface at residual state of NSF-clay (σ_V = 50 kPa, V = 0.5 mm/min)

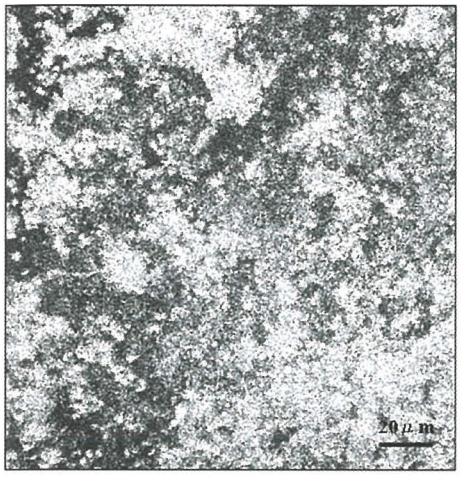

FIG. 10. The planar image of the contact part of the shear surface and the glass

water for comparison. The spectrum of bulk water was measured bulk water in glass sell. The fine peak group between 3500 cm^{-1}–3900 cm^{-1} is absorption of steam and the broad peak around 3400 cm^{-1} is OH stretching vibration of the adsorbed water near the shear surface of NSF-clay. From the figure, we can see that the spectrum of the adsorbed water of a shear surface and that of bulk water are similar. The infrared spectrum of NSF-clay, when changing the contact pressure of ATR prism from 10 kPa to 40 kPa, is shown in Fig. 12-b. It is recognized that the absorbance of OH stretching vibration (around 3400 cm^{-1}) of adsorbed water was decreasing with the increase in the contact pressure of ATR prism. It is thought to show the dehydration from the shear surface.

DISCUSSION

From these analyses, we discuss the shear phenomenon at the residual state of clay. This paper describes the shear prop-

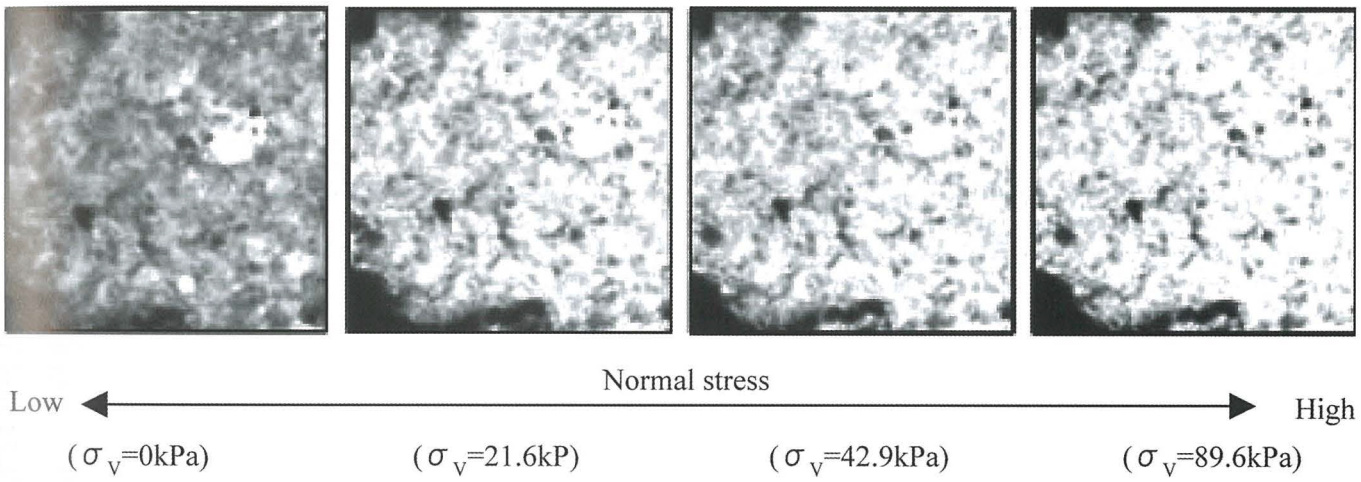

FIG. 11. The change in the CLSM image of NSF-clay as the increase in the normal stress (170 μm × 170 μm)

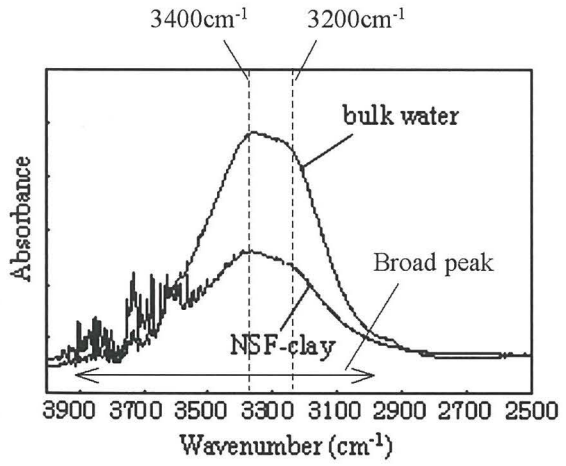

(a) Adsorbed water of shear surface and bulk water

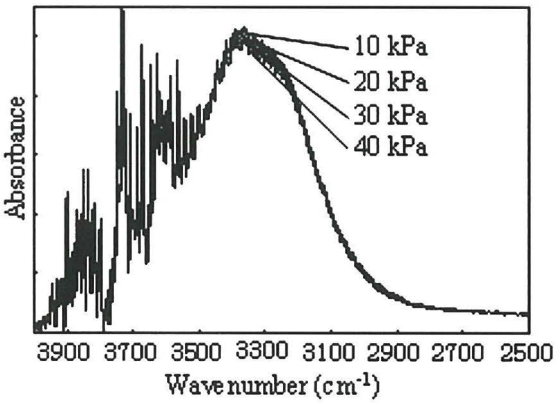

(b) NSF-clay when changing the contact pressure of the ATR prism

FIG. 12. The infrared spectrum of adsorbed water on shear surface

erty at the residual state in relation to a basic concept based on tribology. The reason why tribology and colloidal chemistry were introduced in this study stems from the understanding that the shear phenomenon at the residual state is "friction phenomenon."

Friction surface

Friction phenomena due to contact between two surfaces involve a "contact between solid bodies" problem. A solid surface such as metal contains various irregularities depending on scales at the shear surface, which requires us to distinguish between "apparent contact area" and "real contact area" by Holm (1958). What is important to friction force is the summation of actual contact points (minute contact points) where the contact between protrusions on respective surfaces takes place (Fig. 13). At the plastic contact of clay materials, the actual contact area is in proportion to the external load (Bowden & Tabor, 1964; Greenwood & Williamson, 1966).

The shear surface which looked flat to the naked eye was actually not completely flat microscopically, and by AFM, it became clear to have concavity and convexity. Moreover, it was realized that the area of contact part becomes larger with the increase in normal stress by CLSM. This result was the same as that of the friction mechanism in elastic bodies, such as metal.

Lubrication state at friction surface

Tribology shows that actual contact area depends on state of lubrication between solid surfaces. As clarified in Fig. 7, the residual strength refers to the state of lubrication by water at the shear surface. Conditions between solid surfaces produce various phenomena depending on (1) properties of the lubricating film, (2) load, and (3) shear velocity at contact area and are summarized into three regions as follows by Stribeck (1902) (Fig. 14-a).

"Boundary lubrication" involves a thin lubricating film of several molecular layers or less, partly with solid contact at protrusions. In its friction property, interactions at solid contacts and between solid-fluid film, in particular surface chemical reactions and chemical reactivity of the fluid film, are very important. "Fluid lubrication" is the state of two solid surfaces completely separated by the lubricating film. Its friction property is determined by the viscosity or viscoelasticity of the lubricating film. "Mixed lubrication" is a mixed state of fluid lubrication and boundary lubrication (Fig. 15).

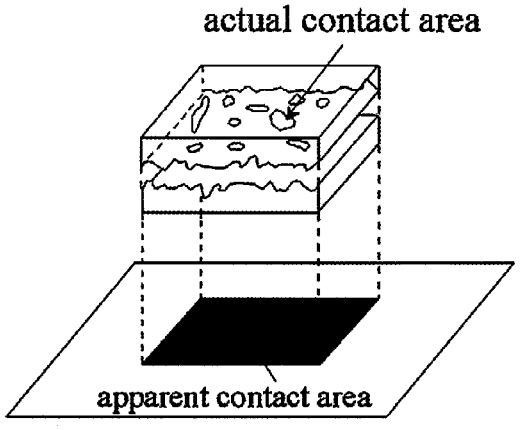

FIG. 13. Conceptual diagram of actual contact area

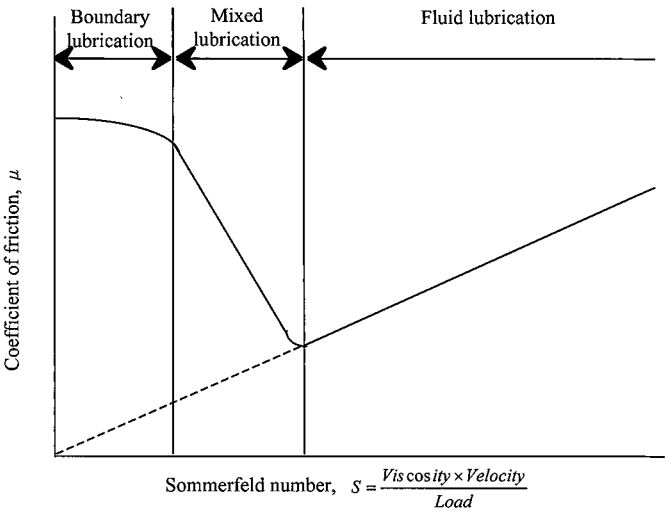

(a) Stribeck curve and three regions of lubrication state (Stribeck, 1902)

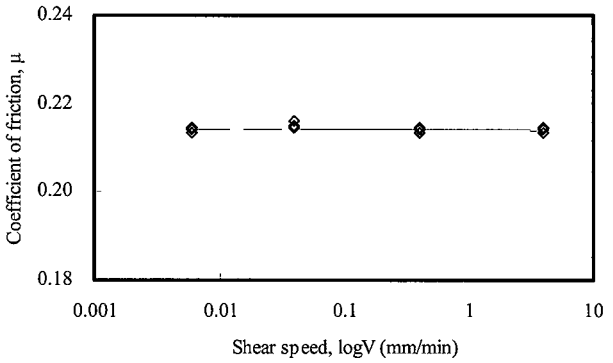

(b) Relationship of Coefficient of friction and Shear speed at the residual state of NSF-clay

FIG. 14. Relationship of experimental value and basic concept in lubrication state

Coefficient of friction μ as shown in Stribeck curve depends or otherwise of the shear velocity according to the circumstance. Coefficient of friction μ do not depend on the shear speed V as shown in Fig. 14-b. And, Mitachi et al. (2003) reports that the residual strength will depend little on the shear velocity. These experimental results suggest that the lubrication state of a shear surface is equivalent to the boundary lubrication. Assuming" that the shear surface consisting of clay materials exists at the boundary lubrication state, mobilization of strength comes from interaction (static electrical force, intermolecular force, and hydrating force) due to surface electrical chemistry of clay minerals. A similar tendency is obtained in the experiment intended for agar gel (Nitta et al., 2003).

In the case of saturated clay, all pores are filled with water, so it is believed that water existing in the non-contact part was observed by CLSM. The infrared spectrum of this water was very similar to that of bulk water, and it was confirmed by FTIR measurement that the water was removed with the

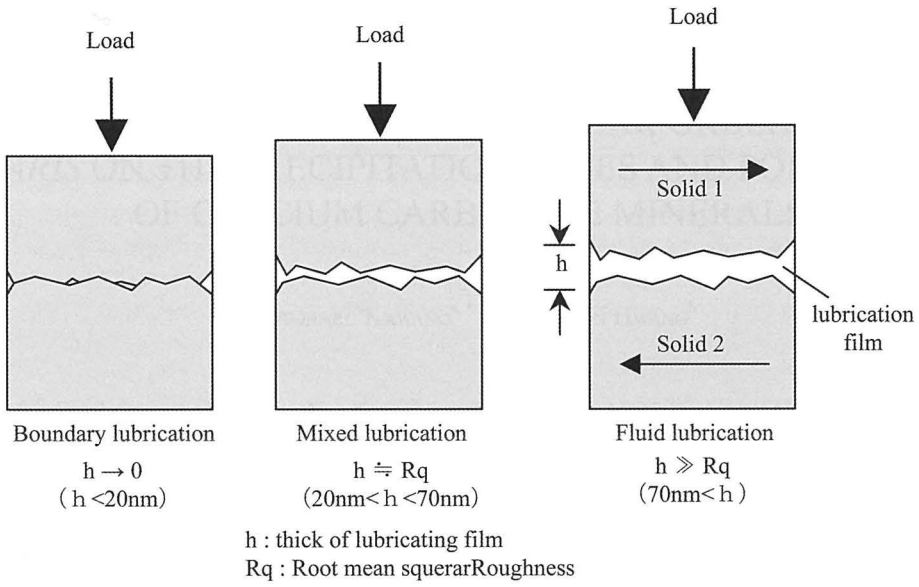

FIG. 15. Mode of friction depending on each lubrication condition

increase in normal stress.

CONCLUSIONS

The following conclusions are obtained.

(1) A shear surface at the residual state was not a perfect flat, but unevenness existed on it according to the AFM observation.

(2) The different light and dark reflection patterns were observed on the contact plane of a glass board and shear surface of NSF-clay by CLSM. It means that the contact part was only partial. Thus the existence of "the actual contact area" was confirmed.

(3) The light parts increased due to the increase in the normal stress by CLSM. This indicates that the actual contact area increased as the normal stress increased.

(4) The spectrum of the adsorbed water of a shear surface and that of bulk water were similar according to the FTIR.

(5) It is recognized that the absorbance of OH stretching vibration (around 3400 cm^{-1}) of adsorbed water was decreasing with the increase in the contact pressure of ATR prism. It is thought to show the dehydration from a shear surface.

REFERENCES

BISHOP, A.W., GREEN, G.E., GARGE, V.K., ANDRESEN, A. and BROWN, J.D. (1971) A new ring shear apparatus and its application to the measurement of residual strength. Geotechnique, **21(4)**, pp.273–328.

BOWDEN, F.P. and TABOR, D. (1964) The friction and lubrication of solids, part 2, Oxford university press.

DERJAGUIN, B.V. and LANDAU, L. (1941) ActaPhysicochim, **14**, 633–662.

GREENWOOD, J.A. and WILLIAMSON, J.B.P. (1966) Proceedings Roy. Soc., **A295**, 300.

HOLM, R. (1958) Electric Contacts Handbook, **3**, Springer 247.

ISRAELACHVILI, J.N. (1992) Intermolecular and surface forces. London: Academic Press.

Japanese Geotechnical Society (1990) Standard lexicon of soil engineering. Tokyo: Japanese Geotechnical Society. (in Japanese)

Japanese Society of Tribologists (ed.) (1995) Tribology Dictionary Tokyo: Yokendo. (in Japanese)

MITACHI, T., OKAWARA, M. and KAWAGUCHI, T. (1999) Method for determining design strength parameters for slope stability analysis, Proc. of International Symposium on Slope Stability Engineering, IS-Shikoku'99: 781–785.

MITACHI, T., KUDA, T., OKAWARA, M., and ISHIBASHI, M. (2003) Determination of strength parameters for landslide slope stability analysis by laboratory test and inverse calculation engagement. *Jounal of the Japan Landslide Society*, **40(2)**, 105–116.

OECD, Research Group on Wear of Engineering Materials (1969) Glossary of terms and definitions in the field of friction, Wear and Lubrication –Tribology–, OECD.

OKAWARA, M., KABUTOYA, N. and MITACHI, T. (2002) On the method of long displacement box shear test for residual strength measuring of clay. Proc. 37th Japan national conf. on geotechnical engineering, 219–220. (in Japanese)

OKAWARA, M. and MITACHI, T. (2003) Basic research on mechanism of the residual strength of clay, Proceedings of the Third International Symposium on Deformation Characteristics of Geomaterials, IS Lyon, 505–510.

SKEMPTON, A.W. (1964) Long-term stability of clay slopes. *Geotechnique*, **14(2)**, 77–102.

SKEMPTON, A.W. (1985) Residual strength of clays in landslides, foiled strata and the laboratory. *Geotechnique*, **35(1)**, 3–18.

STRIBECK, R. (1902) Z. des VDI, 46.

TANAKA, K. (1995) The story of friction. Tokyo: Japanese Standerds Association. (in Japanese)

UESUGI, M. and KISHIDA, H. (1986) Frictional resistance at yield between dry sand and mild steel. *Solis and Foundations*, **26(4)**, 139–149.

VERWEY, E.J.W. and OVERBEEK, J.Th.G. (1948) Theory of Stability of Lyophobic Colloids, Amesterdam: Elsevier.

YAMASAKI, T. (2000) Research on structure of shear zone in re-movement type landslides and soil properties, doctoral thesis, Saga University, Japan. (in Japanese)

NITTA, T., ENDO, Y., HAGA, H. and KAWABATA, K. (2003) Microdomain structure of agar gels observed by mechanical-scanning probe microscopy. *Journal of Electron Microscopy*, **52(3)**, 277–281.

TALLIAN, T.E. (1967) On Competing Failure Modes in Rolling Contact. *ASLE TRAMACTIONS*, **10**, 418–438.

Hashimoto, H. (2006) Tribology, Morikita Publishing Co., Ltd. (in Japanese)

Hisatsune, T., Okawara, M., and Mitachi, T. (2008) Measurements of Frictional Force and Coefficient of Viscosity of Pure Clay Minerals under the Different Temperature Conditions using AFM, Proc. 48th Hokkaido conf. on geotechnical engineering, **48**, 361–364. (in Japanese)